RESEARCH ARTICLE

ENVIRONMENTAL MICROBIOLOGY · Applied Microbiology International

Seasonal shifts in community composition and proteome expression in a sulphur-cycling cyanobacterial mat

Sharon L. Grim[1] | **Dack G. Stuart**[2] | **Phoebe Aron**[1] | **Naomi E. Levin**[1] |
Lauren Kinsman-Costello[3] | **Jacob R. Waldbauer**[4] | **Gregory J. Dick**[5]

[1]Department of Earth and Environmental Sciences, University of Michigan, Ann Arbor, Michigan, USA

[2]Cooperative Institute for Great Lakes Research, University of Michigan, Ann Arbor, Michigan, USA

[3]Department of Biological Sciences, Kent State University, Kent, Ohio, USA

[4]Department of the Geophysical Sciences, University of Chicago, Chicago, Illinois, USA

[5]Department of Earth and Environmental Sciences, Cooperative Institute for Great Lakes Research, University of Michigan, Ann Arbor, Michigan, USA

Correspondence
Gregory J. Dick and Sharon L. Grim, Department of Earth and Environmental Sciences, University of Michigan, 1100 North University Avenue, Ann Arbor, MI 48109, USA.
Email: gdick@umich.edu and sgrim@umich.edu

Present addresses
Sharon L. Grim, Woods Hole Oceanographic Institution, Woods Hole, Massachusetts, USA; Dack G. Stuart, Woods Hole Group, Bourne, Massachusetts, USA; and Phoebe Aron, Hazen and Sawyer, Baltimore, Maryland, USA.

Abstract
Seasonal changes in light and physicochemical conditions have strong impacts on cyanobacteria, but how they affect community structure, metabolism, and biogeochemistry of cyanobacterial mats remains unclear. Light may be particularly influential for cyanobacterial mats exposed to sulphide by altering the balance of oxygenic photosynthesis and sulphide-driven anoxygenic photosynthesis. We studied temporal shifts in irradiance, water chemistry, and community structure and function of microbial mats in the Middle Island Sinkhole (MIS), where anoxic and sulphate-rich groundwater provides habitat for cyanobacteria that conduct both oxygenic and anoxygenic photosynthesis. Seasonal changes in light and groundwater chemistry were accompanied by shifts in bacterial community composition, with a succession of dominant cyanobacteria from *Phormidium* to *Planktothrix*, and an increase in diatoms, sulphur-oxidizing bacteria, and sulphate-reducing bacteria from summer to autumn. Differential abundance of cyanobacterial light-harvesting proteins likely reflects a physiological response of cyanobacteria to light level. *Beggiatoa* sulphur oxidation proteins were more abundant in autumn. Correlated abundances of taxa through time suggest interactions between sulphur oxidizers and sulphate reducers, sulphate reducers and heterotrophs, and cyanobacteria and heterotrophs. These results support the conclusion that seasonal change, including light availability, has a strong influence on community composition and biogeochemical cycling of sulphur and O_2 in cyanobacterial mats.

INTRODUCTION

The innovation of oxygenic photosynthesis (OP) by cyanobacteria shaped the geosphere and biosphere by driving the rise of oxygen ∼2.4 billion years ago (Lyons et al., 2014). In modern systems, cyanobacteria are a core constituent of photosynthetic microbial mats by providing organic matter, fixed nitrogen, and O_2 for diverse communities (Bolhuis et al., 2014; Stal, 2012). These cyanobacterial products stimulate the metabolism of other microbes such as sulphate-reducing bacteria (SRB), sulphide-oxidizing bacteria, and methanogens, which contribute to biogeochemical fluxes of gasses such as methane and sulphide (Hoehler et al., 2001).

Some cyanobacteria are also capable of anoxygenic photosynthesis (AP), which uses H_2S as a reductant in place of H_2O and produces S^0 rather than O_2, and can sustain microbial mats in sulphidic conditions that are toxic to most cyanobacteria (Biddanda et al., 2015; Cohen et al., 1975; de Beer et al., 2017; Dick et al., 2018; Klatt, Meyer, et al., 2016). Sulphidic photic habitats are rare in the modern world but have potential as analogues to understand Earth's biogeochemical evolution (Dick et al., 2018; Lenton & Daines, 2017; Stal, 2012), and to help address open questions about the biological mechanisms underpinning the pattern of Earth's oxygenation (Dick et al., 2018; Hamilton et al., 2016).

Light availability exerts strong control on the composition, physiology, and metabolism of cyanobacterial communities. Cyanobacterial niches are defined in part by adaptations to intensity and wavelength of light (Moore et al., 1998; Oberhaus et al., 2007; Ward et al., 2006). Light availability in microbial mats varies on vertical microscales (Jørgensen et al., 1987) that can influence community composition to an extent comparable to variation across larger geographic spatial scales (Al-Najjar et al., 2014). Ice-covered Antarctic lakes illustrate how variation of light due to ice thickness and water depth shapes which cyanobacteria taxa are present in cyanobacterial mats and their productivity, metabolism, and physical structure (Dillon et al., 2020b; Hawes & Schwarz, 2001; Mackey et al., 2017; Moorhead et al., 1997). Cyanobacteria also respond to changes in light at the cellular level via phototaxis (Richardson & Castenholz, 1987) and by modulating their pigment content (Bryant, 1982; Falkowski & LaRoche, 1991) and proteome (Cobley et al., 2002), especially the amount of light-harvesting phycobiliproteins (Hihara et al., 2001).

Light level is also tightly intertwined with the biogeochemistry of cyanobacterial mats because it governs both rates of photosynthesis and the balance of AP and OP, and thereby O_2 production and H_2S consumption (Dick et al., 2018; Jørgensen et al., 1986; Klatt et al., 2020, 2021). For cyanobacteria capable of both AP and OP, sulphide is often used as the electron donor before water, thus sulphide-driven AP controls OP such that in the presence of sulphide no OP will take place (Klatt et al., 2015). Higher light levels stimulate higher rates of AP and faster depletion of sulphide; if this outpaces the rate of sulphide supply (e.g., from diffusion or local sulphate reduction), then sulphide is exhausted and OP takes over. Hence, oxygenic cyanobacteria may produce oxygen oases in anoxic conditions (Sumner et al., 2015). To date, studies of the effects of light on cyanobacterial mats have focused on geochemical cycling of in situ OP/AP populations on diel scales (Hamilton et al., 2018; Klatt, Meyer, et al., 2016). Nuances observed in diel geochemical cycles can become integrated over longer time scales from seasons to years, and these longer term patterns are more likely to be recorded in geochemical sediment records. However, the responses of cyanobacterial AP and OP dynamics to seasonal changes in light have not been previously documented.

Physical and chemical conditions also influence the abundance and activities of microbes in mat systems (Dillon et al., 2020a; Stal, 2012). Sulphide concentration and temperature shape the relative abundance of primary producers, which can include cyanobacteria, diatoms, and anoxygenic phototrophs (Camacho et al., 2005; Cohen et al., 1975). In turn, the geochemistry of mats is shaped by consortia of tightly interacting organisms. Oxygen and sulphide are required and consumed by sulphur-oxidizing bacteria (SOB), and their concentrations influence competition between SOB and cyanobacteria (Klatt, de Beer, et al., 2016). Sulphate-reducing bacteria (SRB) in cyanobacterial mats (Canfield & Des Marais, 1991; Teske et al., 1998) affect cyanobacterial photosynthesis through local production of sulphide (de Beer et al., 2017; Hamilton et al., 2018). Seasonal cycles can shift the delivery of nutrients and light to microbial populations (Bolhuis et al., 2014) and influence microbial mat community composition (Cardoso et al., 2019; Pinckney et al., 1995). In other cases, cyanobacterial mat communities show remarkable resilience to seasonal and climatic change through physiological plasticity (Aguilera et al., 2020; Lionard et al., 2012). The effects of seasonally changing light on the chemistry, composition, and function of redox-stratified microbial mat communities, where light is expected to shape the balance of OP and AP and thus concentrations of oxygen and sulphide, are largely unknown.

The Middle Island Sinkhole (MIS) in Lake Huron hosts extensive cyanobacterial mat communities that sit at an O_2/H_2S interface and switch between OP and AP depending on supply of sulphide (Kinsman-Costello et al., 2017; Voorhies et al., 2012). The mats are bathed in low-oxygen, high-sulphate groundwater that has relatively stable temperature throughout the year (Ruberg et al., 2008), providing an opportunity to study the relationship between seasonal changes in light and groundwater chemistry and microbial community composition and function. To test the hypothesis that light has strong effects on microbial mat community composition and metabolism, we measured light and groundwater chemistry and conducted 16S rRNA gene sequencing and proteomics in samples collected between June and September from 2009 to 2015. We observed strong shifts in the community structure and function of cyanobacteria and sulphur-cycling bacteria, revealing large seasonal impacts on both phototrophs and their metabolic partners.

EXPERIMENTAL PROCEDURES

Sample collection

We sampled the microbial community of MIS (located at 45° 11.914 N, 83° 19.671 W), a sinkhole of ~23 m depth below water surface, 125 m length, and 100 m width in Lake Huron (Baskaran et al., 2016; Kinsman-Costello et al., 2017; Ruberg et al., 2008). Samples were collected once in 2009, and one to three times a year between 2011 and 2015 during the day between 9 AM and 3 PM when conditions and personnel safety permitted collection. Scuba divers from the NOAA Thunder Bay National Marine Sanctuary used 20 × 7 cm clear polycarbonate tubes and rubber stoppers to collect intact flat purple mat (Figure S1) and sediment cores from the central region of the sinkhole, hereafter referred to as the 'arena' (Figure S2). Cores were kept upright, in the dark, and on ice or at 4°C until they were sampled within 48 h of collection. Microbial mat, which was located within the first 1.0 mm of the core surface with sediment sparsely distributed and was not firmly attached to the sediment underneath (Merz et al., 2021; Voorhies et al., 2012), was removed intact from cores, homogenized, stored in 2 mL microcentrifuge tubes, and frozen at -80°C until DNA or protein extraction.

Physicochemical measurements

To measure photosynthetically available radiation (PAR) at 23 m depth in the sinkhole, we used a LiCor LI-192 underwater quantum sensor (LiCor Biotechnology; sampled in 2009–2013 and 2017), a compact optical profiling system for UV light in natural waters (UV C-OPS; Biospherical Instruments Inc.; Cory et al., 2016, in 2014), a hyperspectral profiler (HyperPro II profiler, Sea-Bird; 2015–2016), and HOBO loggers mounted 0.25–0.75 m above the sediment surface (Onset Computer Corporation; in 2014–2017). HOBO logger light measurements were calibrated to PAR quantitation through hyperspectral profiling of the 23 m-deep light field at the same time as the loggers. For each month, an average and quartiles of maximum daily light intensity were calculated from the summarized daily maxima and the episodic measurements. k-attenuation coefficients (m^{-1}) were calculated from the linear relationship,

$$\ln(I_{23}) = \ln(I_D) - k(D - 23)$$

where I is irradiance (μmol photon $m^{-2}\,s^{-1}$) at the last measured depth D in meters in vertical profiles obtained through LiCor, C-OPs, and HyperPro II instruments. These k values were used to project HOBO-acquired values to uniform depth at 23 m.

Groundwater for conductivity and water stable isotope measurements was collected by divers with 60 mL syringes at specific locations in the sinkhole. These elemental and stable isotope measurements permitted the calculation of a linear mixing model of water sources in the MIS. Specific conductivity in 2014–2018 was measured using a handheld probe (Yellow Springs Instruments Inc.), as well as calculated from ionic composition. We measured major element anion concentrations in water samples including chloride (Cl^-), fluoride (Fl^-), and sulphate (SO_4^{2-}) using electrolytic-suppression ion chromatography (Dionex, Thermo Scientific; average recovery of standards was 10.3%, 10.6%, and 14.1%, respectively; standards' relative percent differences (RPD) were 11.6%, 23.3%, and 4.6%, respectively). We measured concentrations of major cation elements including calcium (Ca^{2+}), sodium (Na^+), and magnesium (Mg^{2+}) with inductively coupled plasma-optical emission spectroscopy (ICP-OES, Perkin Elmer; average recovery of standards was within 5.2%, 12.6%, and 4.7%, respectively; and standards' RPDs were 4.8%, 12.7%, and 5.0%, respectively). Sulphate measurements are reported from samples collected in 2012–2013 (Kinsman-Costello et al., 2017), as well as samples newly collected in 2014–2018.

We measured stable oxygen ($^{18}O/^{16}O$) and hydrogen ($^2H/^1H$) isotope ratios ($\delta^{18}O$ and δD) in select samples from 2015 to 2018 to trace the influence of water reservoirs and mixing in the groundwater. Isotopic measurements were performed on a Picarro L2130-i cavity ringdown spectrometer with an A0211 high-precision vaporizer and attached autosampler (Picarro). The Picarro ChemCorrect software was used to monitor samples for organic contamination. Precision was better than 0.1‰ and 0.3‰ for $\delta^{18}O$ and δD, respectively, based on replicate injections of deionized water. Data are reported as δ values relative to the Vienna standard mean ocean water normalized to standard light Antarctic precipitation (VSMOW-SLAP; Coplen, 1996). Globally, the relationship between $\delta^{18}O$ and δD values of meteoric waters is characterized by the Global Meteoric Water Line (Craig 1961), where,

$$\delta D = 8.0 \times \delta^{18}O + 10$$

The deviation from global water patterns is labelled the deuterium-excess (d-excess):

$$d - \text{excess} = \delta D - 8.0 \times \delta^{18}O$$

The average d-excess for the Great Lakes is $+3.2$‰, reported as the intercept in the Great Lakes Mean Water Line (GLWL; Jasechko et al., 2014). $\delta^{18}O$ and δD values of this study's water samples were

compared with available data from Lake Huron (Jasechko et al., 2014), Michigan groundwaters (Bowen et al., 2012) located within 100 km of the sinkhole, and sinkholes offshore of Alpena, including MIS (Baskaran et al., 2016). We used the compositions of the Alpena library fountain, which taps the putative source of MIS groundwater based on its source depth (Ruberg et al., 2008), and surface water samples from Lake Huron as endpoints of a linear mixing model to explain the observed isotopic values in these water samples.

DNA preparation and sequencing

We extracted up to 0.5 g of wet mat material using a modified version of the MPBio Fast DNA Spin Kit for Soil (MP Biomedical, Santa Anna, CA) as described in Voorhies et al. (2012). Amplicon libraries were prepared and sequenced on an Illumina MiSeq at the University of Michigan Host Microbiome Core using standard methods (Kozich et al., 2013; Seekatz et al., 2015) and bacterial primers 515F/806R for amplification of the 16S rRNA gene v4 region. Sequences can be obtained from NCBI Sequence Read Archive (SRA-SRP067517).

Quantitative proteomics

Protein abundances in replicate samples from June ($n = 3$), July ($n = 4$), and October ($n = 3$) 2015 were evaluated using diDO-IPTL isobaric peptide labelling (Waldbauer et al., 2017). From 0.25 to 5.0 g of wet mat material, proteins were extracted in a denaturing and reducing buffer (1% SDS, 10% glycerol, 10 mM dithiothreitol, 200 mM Tris, pH 8) using heat (95°C, 20 min) and sonication (QSonica Q500). Cysteines were alkylated by addition of iodoacetamide (40 mM, 30 min dark). Following centrifugation to pellet mineral material, proteins were precipitated in acetone (−20°C, overnight) and pelleted by centrifugation. Protein pellets were redissolved in 8 M urea and purified by a modified eFASP (enhanced filter-aided sample preparation) protocol (Erde et al., 2014), digested with MS-grade trypsin (Thermo Pierce) at 37°C overnight, and peptides were eluted and dried by vacuum centrifugation. diDO-IPTL isobaric labelling, wherein peptide N-termini are d_2/d_0-dimethylated and C-terminal oxygens exchanged with $^{16}O/^{18}O$-water (Waldbauer et al., 2017), is described in detail at protocols.io (https://doi.org/10.17504/protocols.io.d2i8cd). An internal standard composed of pooled $d_0/^{18}O$-labelled aliquots of all samples was used for quantitative comparisons. This standardization normalizes for different bulk sample masses and overall protein extraction/digestion efficiencies. For liquid chromatography-mass spectrometry analysis, peptide samples were separated on a monolithic capillary C18 column (GL Sciences Monocap Ultra, 100 μm I.D. × 200 cm length) using a water-acetonitrile +0.1% formic acid gradient (2%–50% AcN over 180 min) at 360 nL/min using a Dionex Ultimate 3000 LC system with nanoelectrospray ionization (Proxeon Nanospray Flex source). Mass spectra were collected on an Orbitrap Elite mass spectrometer (Thermo) operating in a data-dependent acquisition mode, with one high-resolution (120,000 $m/\Delta m$) MS1 parent ion full scan triggering Rapid-mode 15 MS2 CID fragment ion scans of selected precursors. IPTL mass spectral data were analysed using MorpheusFromAnotherPlace (Waldbauer et al., 2017). Proteomic mass spectral data are available via ProteomeXchange under accession number PXD031126 and the MassIVE repository (http://massive.ucsd.edu) under accession number MSV000088706 (username for reviewers, MSV000088706_reviewer; password, a).

We used protein sequences predicted from previously generated metagenomes (Grim et al., 2021; Voorhies et al., 2016) to identify proteins, and metagenome-assembled genomic bins refined through anvi'o (Eren et al., 2015) to link proteins to specific organisms. Analysis of the metagenome-assembled genomic bins (MAGs) is described in Grim et al. (2021). Our oscillatorial cyanobacterial bins had 70.4% completion/56.3% redundancy (*Phormidium*, 11.0 Mbp), 91.6%/42.3% (*Planktothrix*, 5.7 Mbp), 95.8%/11.3% (*Pseudanabaena*, 4.3 Mbp), and 22.5%/1.41% (*Spirulina*, 1.1 Mbp), as well as a 527 Kbp collection of cyanobacterial scaffolds that were not able to be confidently binned. Additional bins of interest are listed in Table S1. Metagenomic scaffolds are available through IMG via genome IDs 3300002026 (5000 bp and longer scaffolds), 3300002027 (1500–4999 bp scaffolds), and 3300002024 (1000–1499 bp scaffolds).

16S rRNA gene bioinformatic analysis

Raw pairs of sequencing reads (250 bp) were quality trimmed and merged using 'iu-merge-pairs' within illumina-utils (https://github.com/merenlab/illumina-utils; Eren et al., 2013), using minimum quality score of 25, minimum overlap of 200 bp. At points of divergence in the overlap the higher quality basecall was retained. Merged reads with five or fewer mismatches were kept for Minimum Entropy Decomposition v. 2.1 (Eren et al., 2014) to generate amplicon sequence variants (ASVs) using the following parameters: -d 4 -N 3 --min-substantive-abundance 5 -V 3 --relocate-outliers. We used GAST (Huse et al., 2008) to call taxonomy using the curated SILVA database, and confirmed with BLASTN against SILVA 123 (Pruesse et al., 2007) (bacteria and archaea), and PhytoRef (Decelle et al., 2015) (chloroplasts). mothur v. 1.33 (Schloss et al., 2009) was used to check for chimeras de novo, and putatively chimeric ASVs that did not have

taxonomy assigned via SILVA 123 and GAST were removed. Table S2 provides a summary of sequencing results. We documented the presence of sulphate-reducing genera (e.g. *Desulfonema*, *Desulfobacula*, *Desulfocapsa*, and *Desulfotalea*) in the Thermodesulfo-bacteria through a taxonomic search. The read analysis is outlined here: https://hackmd.io/s/r1CGeQs_G.

Statistical analyses

We used the R statistical environment (R Core Team, 2015) in RStudio (RStudio Team, 2014) to analyse ASVs and proteins. To evaluate similarity in bacterial community composition, we used Morisita-Horn metric to calculate a distance matrix on Hellinger-transformed bacterial relative abundances, as input for nonmetric multidimensional scaling with autotransformation = TRUE. For correlation network analyses, we retained bacterial genera that were at least 0.1% of the total bacterial community ($n = 67$). The genera read counts were used as input to CoNe-tinR (Faust & Raes, 2016) to generate three correlation network matrices using Spearman's rho correlation, Pearson correlation, and Bray–Curtis, implementing the ReBoot procedure as described in the original CoNet (Faust & Raes, 2012) and Benjamini–Hochberg false discovery rate correction, to keep correlations $p < 0.001$. Independently of the CoNet software, we generated one network using *rcorr* on a Bray–Curtis distance matrix calculated from the read counts of genera, and after a Benjamini–Hochberg false discovery rate correction, we retained all correlations $p < 0.001$. The final correlation network contained ASVs and edges whose direction of correlation was supported by all four matrices, with the edges representing the average of the measures. The Bray–Curtis matrices measure community dissimilarity, whereas the other two matrices better detect correlations (Faust & Raes, 2012). Concordance between these matrices retained only positive correlations. Such statistical processing likely reduces the impact of taxonomic bias skewing differential abundance analyses (McLaren et al., 2022). The final network was visualized in Gephi and in a correlogram via corrplot, with the standard deviation (SD) of the mean in the lower triangle. We used analysis of molecular variance (AMOVA) (Excoffier et al., 1992) in the R package *pegas* (Paradis, 2010) on Morisita-Horn transformed relative abundances of genera for testing significant differences in bacterial community structure between months and seasons, and LEFSE in the Galaxy Project (Afgan et al., 2018) on genera relative abundances to identify taxa as biomarkers for seasons and months; those taxa are indicated with significance values. For the evaluation of differential abundance of proteins between seasons, we calculated the weighted mean and weighted SD of

the log$_2$-normalized abundance ratios of samples taken from the same month. Paired *t*-tests ($p < 0.05$) corrected with Benjamini–Hochberg false discovery rate were used to retain significantly different weighted mean abundances.

RESULTS

Seasonal light dynamics

PAR measurements over several years showed that *k*-extinction coefficients ranged from 0.12 to 0.14, were not related to season, and were consistent with previous measurements in Lake Huron (Yousef et al., 2017). During observations of the microbial mats, which were limited to months May–June (hereafter referred to as 'spring'), July–August ('summer'), and September–October ('autumn'), PAR was generally highest in July and lowest in May and October (Figure 1). In addition to the expected astronomical variation of solar radiation, these measurements also reflect varying turbidity in the water column due to phytoplankton growth, and episodic shading from clouds.

The quality of light also varied between seasons. Hyperspectral profiling showed that blue-green light was most available at 23 m depth in the MIS arena (Figure S3) and was directly related to overall PAR
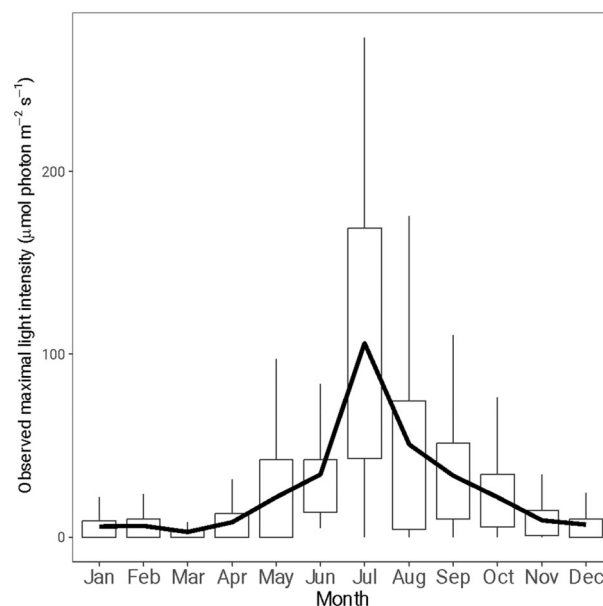
FIGURE 1 Maximal daily light observed each month in the sinkhole above microbial mats. For each month, daily maximum light values from logged data at 23 m depth (2014–2017) and recorded light from episodic measurements to 23 m depth (2009–2016; grey transparent circles) were summarized in box and whisker plots and averaged per month. Boxes represent the 25th–75th percentiles with whiskers covering the minimum and maximum values. The average is plotted with the thick line.

availability. We observed subtle differences in availability of other wavelengths of light indicating green light is more rapidly attenuated in the water column in summer than in the other seasons (Figure S4 and Table S3). Energy in the red wavelengths was generally below $0.002 \, \mu mol \, m^{-2} \, s^{-1}$. Hyperspectral profiles ($n = 2$) outside of the sinkhole (Kinsman-Costello et al., 2017) were comparable to those in the sinkhole, indicating similar water column dynamics between the two sites.

Seasonal variation of groundwater chemistry

Groundwater that vents from its main source, the sinkhole alcove, is thermally and chemically distinct from overlying Lake Huron water, and as it flows through the sinkhole it slowly mixes with lake water (Baskaran

et al., 2016; Ruberg et al., 2008). The conductivity of the dominant source of groundwater (hereafter referred to as 'alcove groundwater source') was on average $3111 \, \mu S \, cm^{-1}$, and it attenuated to an average of $1909 \, \mu S \, cm^{-1}$ as it distributed in the bowl-shaped arena of the sinkhole (hereafter referred to as "MIS arena water"; Table S4 and Figure S5). These values are higher than lake surface water ($208 \, \mu S \, cm^{-1}$), similar to previously reported values for MIS (Baskaran et al., 2016), and lower than the Alpena fountain, which averaged $3457 \, \mu S \, cm^{-1}$ and is thought to reflect the chemistry of source groundwater without any mixing.

The isotopic composition of water samples from the MIS alcove and arena was depleted in both ^{18}O and D compared with lake surface (Table S5 and Figure 2). Isotopic composition of surface waters sampled in this study is presented as averages (± 1 SD) and was indistinguishable from previous measurements of Lake
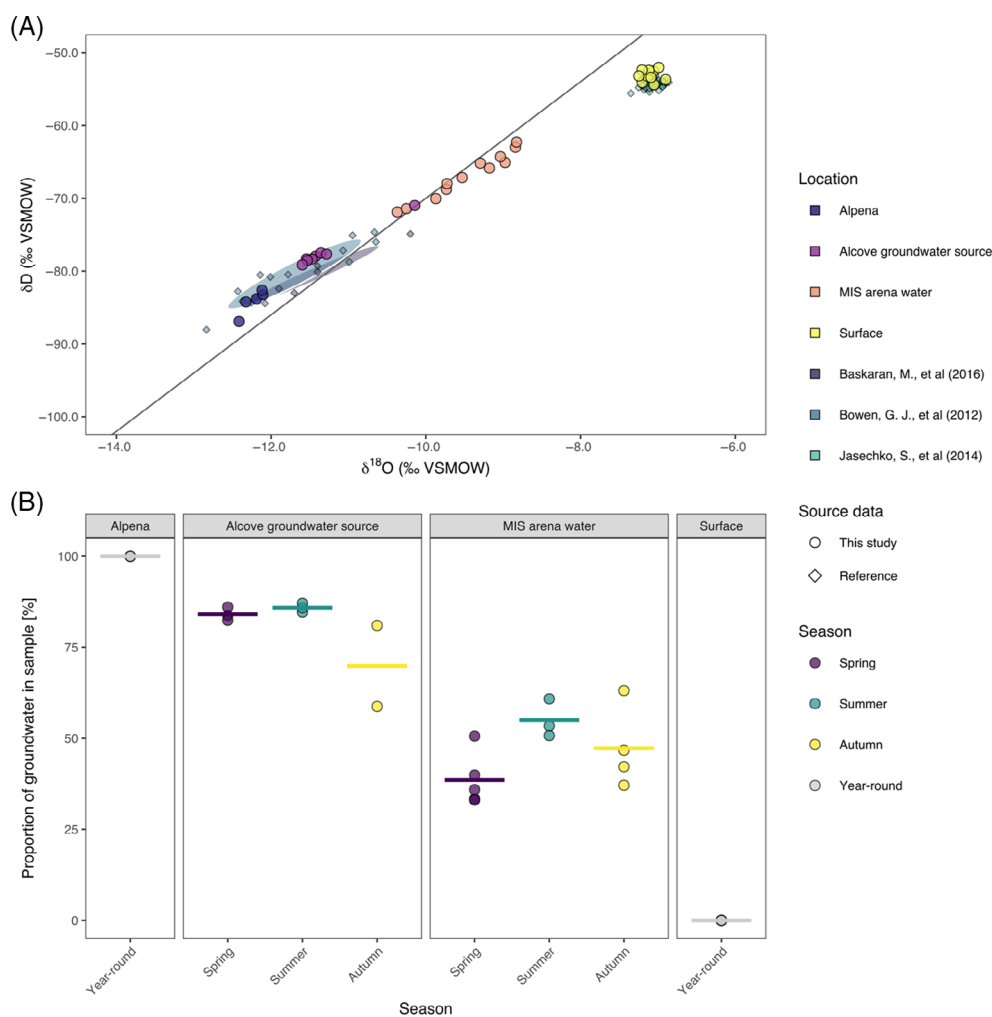
FIGURE 2 Measured values of δD and δ^{18}O and estimated proportion of groundwater in water samples. (A) Isotopic compositions of samples from this study are plotted as circles and coloured by location. Samples from other references are plotted as diamonds, and coloured by study. (B) The average δ^{18}O values for Alpena fountain and surface were used as end-members in a linear mixing model to estimate the proportion of ground water in each sample. Isotopic compositions of samples from this study are plotted as circles and coloured by season. The horizontal line represents the average proportion of groundwater in each season per location. VSMOW, Vienna standard mean ocean water.

Huron water samples (Figure 2A; Jasechko et al., 2014). Additionally, Alpena fountain and alcove groundwater samples were isotopically similar to groundwaters within 100 km of the sinkhole (Bowen et al., 2012) and submerged sinkholes in the immediate area (Baskaran et al., 2016). Year-round $\delta^{18}O$ values for surface waters averaged -7.1 ± 0.1‰, whereas the Alpena fountain averaged -12.2 ± 0.1‰. More seasonal variability was observed in $\delta^{18}O$ measurements from the sinkhole arena and alcove. In arena water samples, the average $\delta^{18}O$ in spring, summer, and autumn were -9.1 ± 0.4‰, -10.0 ± 0.3‰, and -9.6 ± 0.6‰, respectively. In the alcove, across the respective seasons $\delta^{18}O$ averaged -11.4 ± 0.1‰, -11.5 ± 0.1‰, and -10.7 ± 0.8‰. The same regional and seasonal signals were observed in δD measurements. The Alpena fountain samples had substantially lower δD (average: -84.2 ± 1.7‰) compared with the lake surface samples (average: -52.9 ± 0.7‰). Seasonal averages for δD values in arena water samples were -64.8 ± 2.3‰ (spring), -70.1 ± 1.3‰ (summer), and -67.1 ± 3.4‰ (autumn). Alcove water samples had even lower δD values, with seasonal averages of -77.9 ± 0.4‰ (spring), -78.7 ± 0.4‰ (summer), and -74.3 ± 4.7‰ (autumn).

Isotopic compositions can help constrain water sources and influences. In this study, the average d-excess of surface water samples was $+4.2 \pm 0.6$‰, which is slightly higher than the previously reported Lake Huron-specific average d-excess of $+2.6 \pm 1.0$‰ but within the range of measurements for the Great Lakes (Figure S6; Jasechko et al., 2014). Given the sinkhole's proximity to shore, the slightly elevated d-excess values in surface waters likely reflect incomplete mixing of riverine input (d-excess values of rivers in Lake Huron catchment: $+11.3$‰ and $+12.5$‰) and terrestrial runoff (Jasechko et al., 2014). In contrast, d-excess was highest for Alpena fountain samples (average 13.7 ± 0.8‰), which aligns with the d-excess values of terrestrial groundwaters in Michigan's Lower Peninsula most impacted by lake-effect precipitation (Bowen et al., 2012). High d-excess values in the aquifer that sources Alpena fountain (386 m depth below surface) suggest a large contribution of lake-effect precipitation.

We leveraged the $\delta^{18}O$ and δD data to constrain water sources to MIS by constructing a linear mixing model with two isotopic endmembers: the lake surface water samples (no groundwater), and the Alpena library fountain (representing the groundwater reservoir). In the sinkhole arena, the model estimates the proportion of water sourced from the groundwater aquifer increases from spring to summer ($p < 0.03$ by Kruskal–Wallis testing) and decreases summer to autumn ($p < 0.06$; Figure 2B). We observed a similar (though not significant) trend in the alcove source waters, and corroborated the linear mixing model using ion concentrations (SO_4^{2-}, Cl^-, Na^+; Figure S7). Water column

mixing in spring and autumn can lead to a larger input of lake surface water to the sinkhole, yielding higher values of $\delta^{18}O$ and smaller d-excess in the arena. In the summer, lower $\delta^{18}O$ and larger d-excess values in sinkhole arena and alcove waters point to a greater contribution of the groundwater aquifer, likely due to thermal stratification in the water column isolating the cold groundwater layer from surface water.

While the seasonal signal is strong and robust, sampling location may also influence isotopic variability in MIS water. Samples in 2016 were collected in georeferenced locations (Figure S2), whereas in 2015 they were collected opportunistically with sinkhole mat sampling, and in 2017–2018 at one consistent location. Focusing on the georeferenced locations from 2016, the mixing model of isotopic composition suggests that the proportion of aquifer groundwater decreases with greater distance from the alcove source (Figure S2). There are small local sources of groundwater around the circumference of the sinkhole arena (Baskaran et al., 2016), yet the largest source and dominant influence on the isotopic composition is from the alcove groundwater source. Turbulence between the groundwater layer and overlying lake water, and increased distance from the alcove source likely attenuate the signal of aquifer groundwater in arena water samples that are farther from the alcove, yet they are still chemically distinct from surface water and other depths sampled in Lake Huron (Jasechko et al., 2014).

Microbial community structure varies seasonally

We evaluated the bacterial community observed in the microbial mat samples from 2009 to 2015. Samples were categorized as 'spring' (from May and June, $n = 9$), 'summer' (July and August, $n = 13$), and 'autumn' (September–October, $n = 12$). Diatom chloroplast 16S rRNA genes ranged in abundance from 0.14% to 44% (mean ± SD: 12.4% ± 12.7%) of all sequencing reads, belonged primarily to Bacillariophyta; Cymbellaceae, and were removed from further analysis due to the highly variable abundance of 16S rRNA gene copies in their cells (Green, 2011).

Bacterial communities were dissimilar by month (AMOVA, $p < 0.05$) and by season ($p < 0.08$), with spring clustering distinctly from autumn, and summer communities showing a degree of mixing between the two (Figures 3 and S8 and Table S6). Seasonal trends were also apparent in specific taxa, including the dominant cyanobacteria, *Phormidium*, and *Planktothrix* (Figure 4). *Phormidium* was more abundant in summer samples (mean 35 ± SD 24% of the total bacterial community) compared with autumn samples
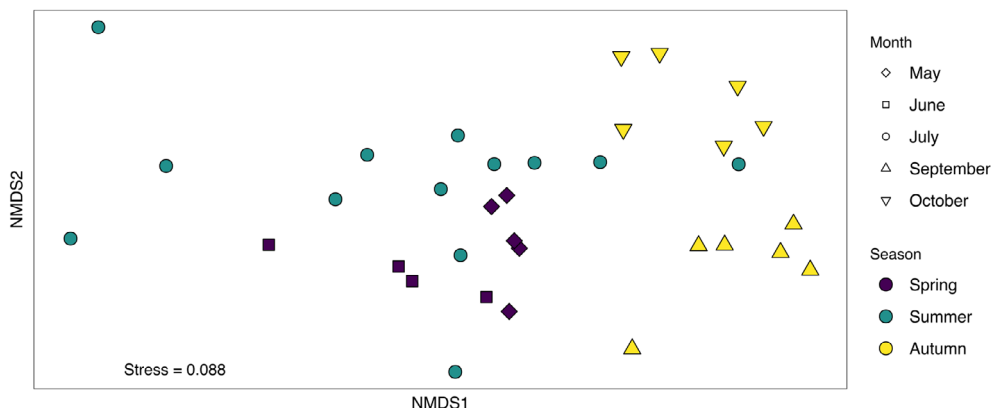
F I G U R E 3 Nonmetric multidimensional scaling (NMDS) plot of bacterial community structure by season, using Morisita–Horn distance matrix calculated from Hellinger-transformed bacterial relative abundances. Samples in May (diamonds) and June (squares) are coloured purple, July samples are green circles, and samples from September (upright triangles), and October (lower triangles) are coloured yellow.
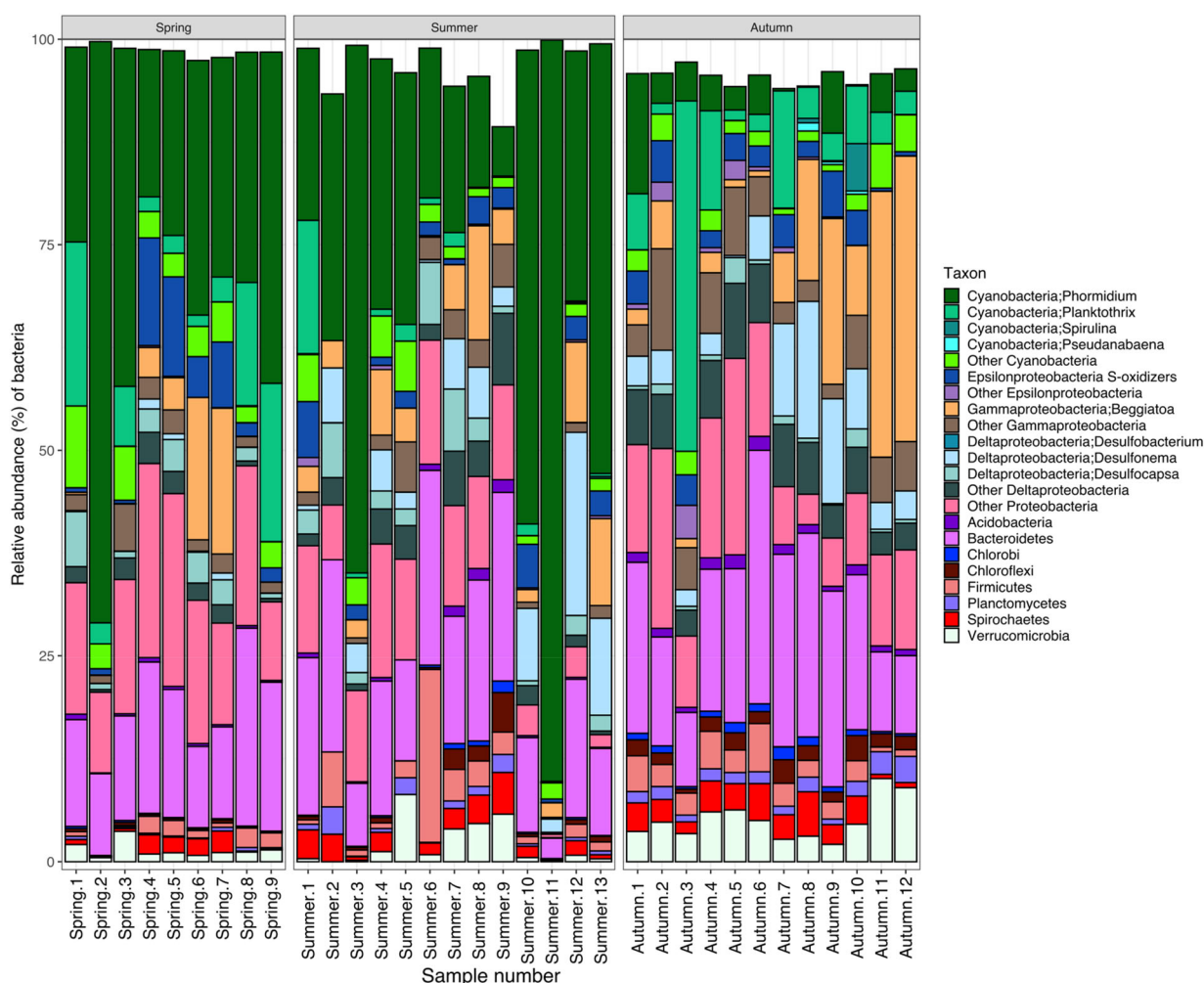
F I G U R E 4 Relative abundance of relevant bacterial taxonomic groups in samples, grouped by season. Sample naming on x-axis reflects chronological order within seasons. After removing non-bacterial reads, samples were normalized to 100%. Relative abundances of key genera were summed and presented, and classes and phyla without those genera are represented.

(mean 4.2% ± 4.0%; LEFSe, *p* < 0.05), whereas *Planktothrix* is more frequently observed in spring and autumn samples (means of 8.0% ± 7.8% and 8.4% ± 11%, compared with 1.9% ± 4.4% in summer; LEFSe, *p* < 0.05; Table S6). Other cyanobacterial taxa were typically 5% or less of the community.

Thermodesulfobacteria, including putative sulphur- and sulphate-reducing bacteria (hereafter "SRB") such as *Desulfonema* and *Desulfocapsa*, ranged from 4.8% ± 0.68% (average of the group's relative abundances ± standard error) of the total bacterial community in spring samples to 12% ± 1.0% and 13% ± 1.7% in summer and autumn (Table S7). Within this group, however, we observed some seasonal peaks in specific genera. Many taxa followed the pattern of *Desulfonema*, which was more abundant in summer and autumn (maximum mean ± SD of 6.0% ± 5.0% compared with 0.34% ± 0.45% in spring, LEFSe, $p < 0.05$). In contrast, *Desulfocapsa* is less abundant in autumn (mean 0.94% ± 0.88% vs. 2.7% ± 2.0% and 3.0% ± 2.6% in spring and summer). Another SRB, *Desulfotalea*, is more abundant in spring (mean 0.002% ± 0.006%) than later months (<0.0001% in summer and autumn).

The most abundant putative sulphur-oxidizing bacteria (hereafter "SOB"), identified by classification in taxonomic groups known to be SOB, were primarily gammaproteobacteria (*Beggiatoa*) and five groups of campylobacteria (*Arcobacter*, *Sulfurospirillum*, *Sulfurovum*, *Sulfuricurvum*, and *Sulfurimonas*). Overall, *Beggiatoa* was at least as abundant (mean ± SD 7.1% ± 8.8%) as putative SOB campylobacteria combined (3.3% ± 3.1%). Other gammaproteobacteria and campylobacterota typically comprised 0%–5% of the community. Other proteobacterial members and Bacteroidetes constituted on average 12% ± 6.2% to 16% ± 6.2% throughout the year. Firmicutes, Spirochaetes, and Verrucomicrobia were each on average 5% or less of the bacterial community. Other bacterial groups, including Acidobacteria, Chloroflexi, Chlorobi, and Planctomycetes, were infrequently observed (<1% typically).

Network analysis identifies taxa with correlated abundances

We used correlation network analysis to understand potential positive and negative relationships between the abundances of 60 bacterial genera in the microbial mat (Figures 5 and S9). All relationships retained were positive in direction and had $r \geq 0.50$. *Beggiatoa* was solely correlated with *Desulfonema*, which was also correlated with *Paludibacter* (Bacteroidetes) and *Desulfobacterium*. *Sulfuricurvum* was linked to other putative sulfide-oxidizing taxa (*Sulfurospirillum*, *Sulfurovum*) as well as the putative SRB *Desulfobacterium*. *Sulfurovum* in turn linked *Sulfurimonas*, *Desulfocapsa*, *Desulfobulbus*, *Desulfomicrobium*, and *Desulfobacula* to the group. *Thiothrix*, another sulphide-oxidizing gammaproteobacterium, was correlated with *Desulfomicrobium*. *Planktothrix*'s sole correlation was with *Paludibacter*. *Phormidium* was not correlated with any taxa.

## Community function differs by season

Quantitative proteomics analyses showed that the abundances of specific proteins belonging to specific genomic bins varied across the seasons (Figure 6 and Table S8). Nearly half (317/789) of proteins identified belonged to cyanobacteria, of which *Phormidium* was
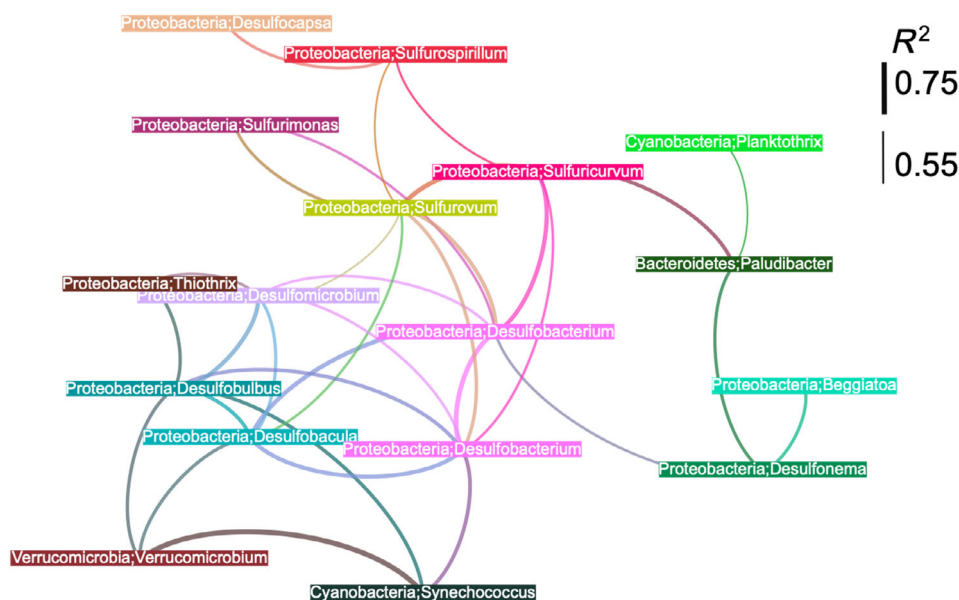
FIGURE 5 Correlation network between relative abundances of key genera. Bray–Curtis distance matrix was calculated from read counts of genera and used to generate a correlation network. Only significant ($p < 0.001$) positive ($r \geq 0.50$) correlations between specific organisms are plotted, and line thickness conveys strength of the correlation. Colours are arbitrary, and line colours are blends of the nodes they connect.

the dominant contributor (215 proteins). Across the entire proteomic dataset, 54% of observed spectra were attributed to phycobilisome-related proteins, with most from *Phormidium* (62%). Based on genome size, redundancy, and completion metrics, there were likely multiple *Phormidium* strains in our MAG bin (Table S1).
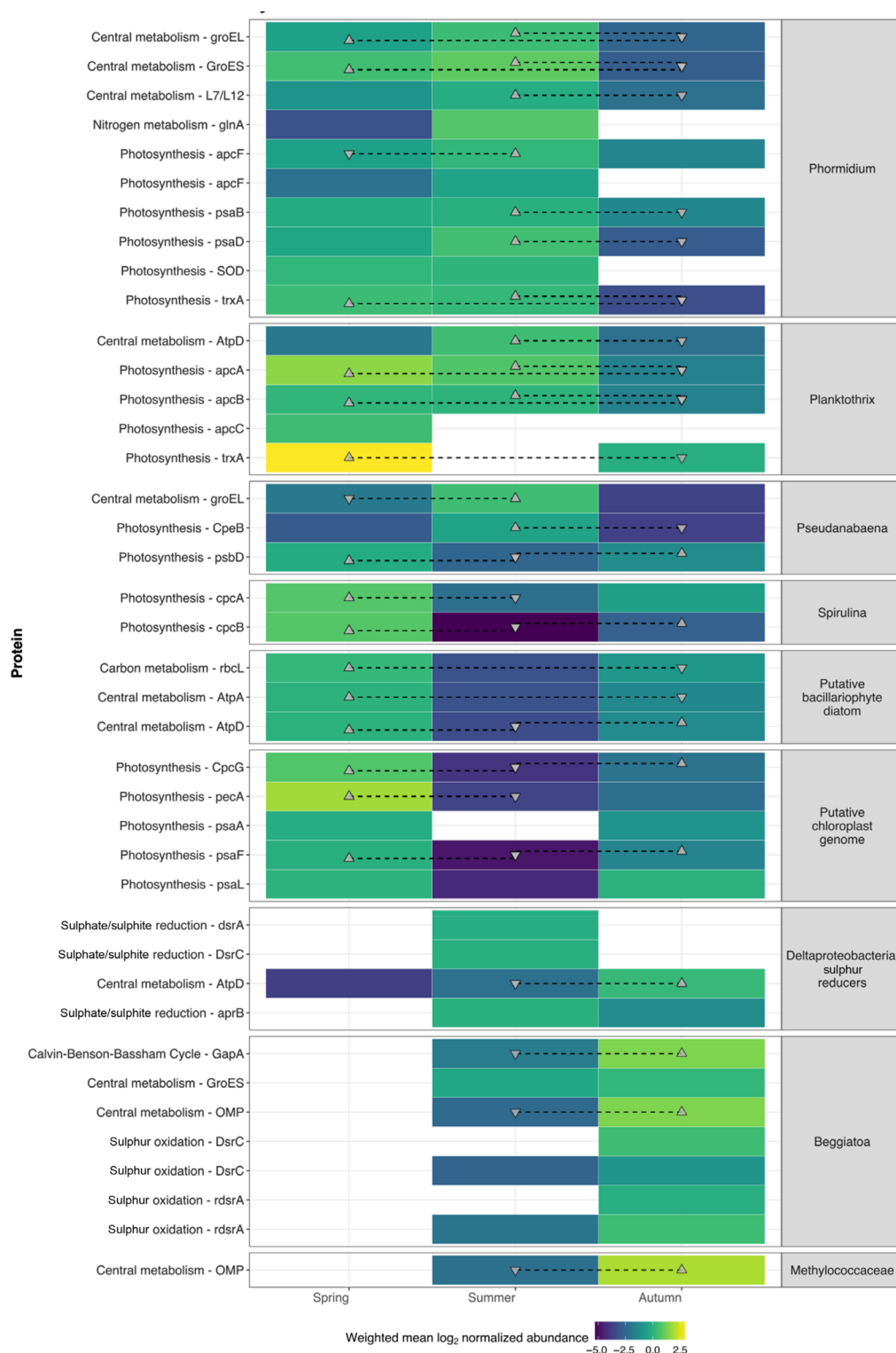
FIGURE 6 Significantly differentially abundant proteins observed in each season. Weighted-mean log$_2$-normalized observations of proteins were used in paired *t*-tests to determine significant changes in abundance. Significant differences in abundances between two season units are indicated with a line between them and the direction of the triangles. For example, a protein significantly abundant in spring versus summer is indicated with an upright triangle in the spring column linked to an upside-down triangle in the summer column. Proteins are grouped by metagenome-assembled genomic bin, and described by function.

We were also unable to resolve several observed proteins to specific MAG bins (referred to as 'unknown organism'). When possible, proteins were assigned taxonomy based on taxonomic profiles of genes from the source contig.

Phormidium dominated the proteins assigned to genome bins in spring and summer (1076/1960 spectra in June and 4269/5535 spectra in July), whereas diatom proteins (Bacillariophyta) were most abundant in autumn (376/1796 spectra observed in September). Despite the dominance of *Phormidium* photosynthetic proteins in the dataset, only a handful varied significantly in abundance between seasons (Table S8). We observed photosystem I proteins PsaB and PsaD in significantly lower abundance in autumn compared with summer. Thioredoxin protein TrxA was significantly less abundant in autumn. An allophycocyanin subunit ApcF protein was less abundant in spring compared with summer. Other phycobilisome proteins composing allophycocyanin, phycoerythrin, and phycocyanin had dynamic abundances across the seasons (Table S8).

Phormidium proteins related to growth also varied in abundance between seasons. Chaperonins GroEL and GroES were significantly less abundant in autumn compared with the other seasons. A ribosomal protein L12 RplL was significantly lower in autumn than in summer. Superoxide dismutase (SOD) and a rhodanese involved in sulphur cycling were abundant exclusively in summer and not observed in other months. Although these SOD and rhodanese proteins are on the same contig as a microaerobic PsbA and a type B sulphide-quinone reductase (Grim & Dick, 2016), we were not able to detect SQR, the sulphide-quinone reductase responsible for AP in cyanobacteria. Further, peptides for *Phormidium*'s photosystem II protein PsbA were not recovered from these samples.

Additional phototrophs, including *Planktothrix*, *Pseudanabaena*, *Spirulina*, other unidentified cyanobacteria, and diatoms, also had photosynthesis- and growth-related proteins that were differentially abundant between seasons, generally higher in summer compared with autumn (Figure 6 and Table S8). This included subunits of accessory pigments allophycocyanin, phycocyanin, phycoerythrin, phycocyanin, and phycoerythrocyanin, thioredoxin, and F0F1-type ATP synthase. Only a few proteins from phototrophs were more abundant in autumn, including a diatom's alpha subunit of F0F1 ATP synthase. Spectral abundance of proteins from *Phormidium* peaked in summer (58.4% of those months' recovered spectra) while *Planktothrix* was responsible for more observed spectra in spring (13.4% of those months' spectra) than in summer and autumn (6.4% each). We observed more MS/MS spectra belonging to diatom PsbA (23 across the dataset) compared with PsaA (6).

Proteins from SOB were generally more abundant in autumn and in some cases only detected in autumn (Table S8). This included *Beggiatoa* proteins for sulphur oxidation (dissimilatory sulphite reductase subunits DsrC and RdsrA), glyceraldehyde 3-phosphate dehydrogenase GapA, and an outer membrane protein. Sulphate-reducing versions of dissimilatory sulphide reductase (DsrA and DsrC) were observed only in summer, and a beta subunit of adenosine-5′-phosphosulfate reductase for dissimilatory sulphate reduction from Desulfobacteraceae was less abundant in autumn compared with summer (Table S8). In contrast, a beta subunit of F0F1 ATP synthase from *Desulfotalea* was significantly more abundant in autumn compared with summer months.

DISCUSSION

Cyanobacterial OP produces O_2 and fixed carbon, providing an energetic and biogeochemical foundation for networks of interacting organisms in microbial mats. Cyanobacterial mats exposed to sulphide also perform AP, producing oxidized sulphur compounds, with the balance of OP and AP being sensitive to irradiance intensity and having major impacts on mat biogeochemistry (Klatt et al., 2015). Here we studied how seasonal changes in light and water chemistry affect microbial community composition and metabolic functions in cyanobacterial mats from MIS over several years. We found that the composition of the microbial community and the proteome of key microbes such as the dominant cyanobacterium (*Phormidium*), the dominant sulphide-oxidizing bacterium (*Beggiatoa*), and a variety of sulphate/sulphur reducing bacteria shifted between seasons (Figure 7). These results are consistent with the hypothesis that seasonal changes in light availability impact sulphur cycling, with more intense sulphur cycling in autumn, when lower light levels should promote more AP and less OP (Klatt et al., 2015, 2021).

We characterized environmental factors that may drive these shifts, focusing on light and groundwater chemistry, which directly influence photosynthesis and sulphate delivery. By altering rates of OP and AP and sulphate reduction, and the abundance of taxa conducting these processes, light and groundwater chemistry are expected to indirectly affect available organic carbon and electron donors (H_2S) and acceptors (O_2 and sulphate). The temperature of groundwater bathing the mats remains 8–10°C through the year, with only transient changes from mixing during storm events (Ruberg et al., 2008). Photosynthetically active irradiance and spectral quality of irradiance varied seasonally (Figures 1, S3, and S4); with green light (which phycoerythrin maximally absorbs) most available in spring and least available in summer likely due to growth of planktonic cyanobacteria in the overlying water (Fahnenstiel & Carrick, 1991). These
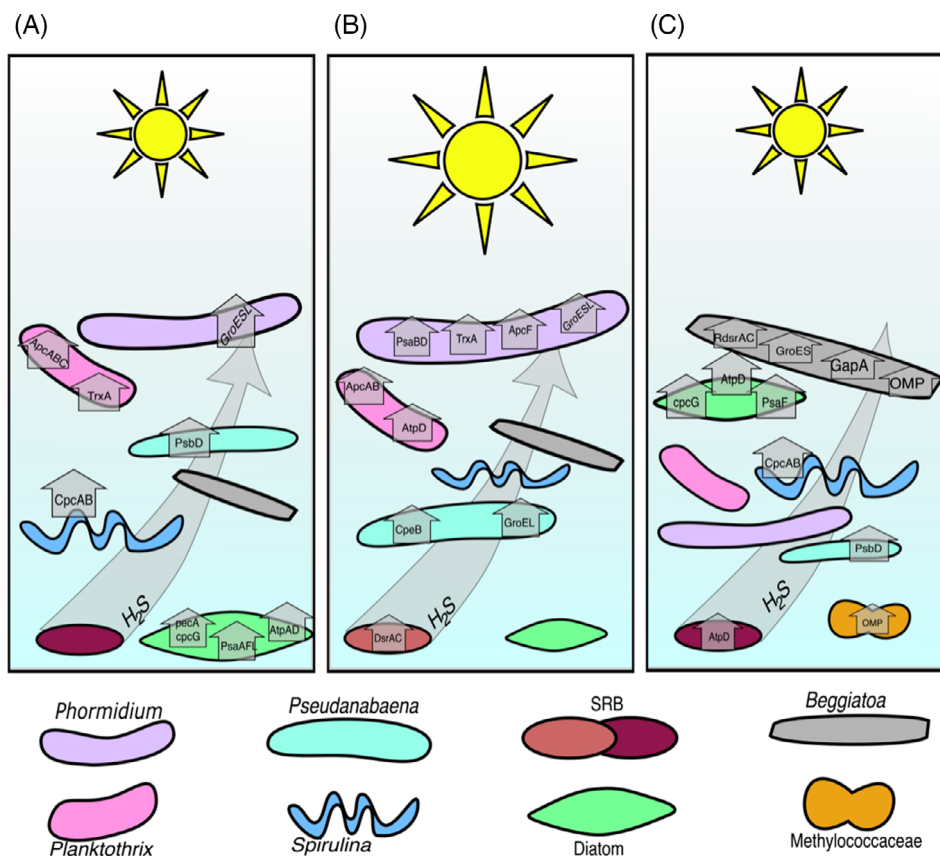
FIGURE 7 Seasonal changes in the functions and membership of the cyanobacterial mat in Middle Island Sinkhole. In spring (A), the microbial community is dominated by cyanobacteria able to thrive at low light (*Planktothrix*, *Pseudanabaena*, and *Spirulina*). In summer (B), though *Planktothrix* and *Pseudanabaena* are still active, *Phormidium* is the most abundant and active cyanobacterium. Different sulphate-reducing bacteria are also active in summer and autumn (C). *Beggiatoa* and Methylococcaceae are abundant and active in autumn. Diatoms are present throughout the year, but their proteins are more abundant in low-light autumn and spring. Vertical placement of microbial members reflects relative depth in the microbial mat.

trends in light quality and quantity are expected to promote modulation of phycoerythrin (which maximally absorbs green light) but not phycocyanin (which maximally absorbs red light) by cyanobacteria, known as group II type complementary chromatic acclimation (De Marsac & Houmard, 1993). These dynamics in light intensity and quality are also likely to differentially affect ecotypes adapted to different light niches (Stomp et al., 2004).

The isotopic and specific conductivity measurements show that the benthic water layer in the sinkhole is composed of seasonally changing proportions of Lake Huron surface water and venting sulphate-rich groundwater. The groundwater source is chemically distinct from the lake surface, and isotopic composition is invariant over the years. Our linear mixing model suggests that groundwater supplies a substantial amount of sulphate to the sinkhole. Over the course of the year, groundwater discharge is higher in summer compared with spring and autumn. Sulphate measurements in overlying groundwater and previously collected samples (Kinsman-Costello et al., 2017) fit

reasonably with predictions from the linear mixing model.

The higher abundance of *Phormidium* in spring and summer than in autumn (Figures 4 and 6) followed light levels and was also reflected in the lower abundance of *Phormidium* proteins for allophycocyanin and photosystem I proteins PsaB and PsaD in autumn. SOD was present in spring and summer but not in autumn, suggesting oxidative stress associated with higher light levels. Seasonal changes in the abundance of other phycobiliproteins were more complex. The *Phormidium* genome bin contained multiple copies of genes for phycoerythrin and phycocyanin, which could result from multiple copies in the genome and/or heterogeneity between strains (Guan et al., 2007; Rinalducci et al., 2008) within the bin (Table S1). The abundance of the different isoforms of these proteins varied through the season (Figure 6), consistent with complementary chromatic acclimation in response to changing light conditions (De Marsac & Houmard, 1993). Variation of phycocyanin and phycoerythrin abundance has also been implicated in photophysiological acclimation

to different light levels in nearby shallow water cyanobacterial mats with similar microbial communities (Snider et al., 2017).

Seasonal differences in the *Phormidium* proteome also indicated broader changes in its physiology. The higher abundance of *Phormidium* ribosomal proteins and GroES/EL proteins in summer likely reflects higher growth rates (Georgopoulos & Welch, 1993; Jahn et al., 2018). Reduced metabolic activity in autumn was also indicated by lower thioredoxin levels. Light energy from photosystem I is used to reduce thioredoxin (TrxA), which interacts with enzymes in the Calvin cycle and oxidative pentose phosphate cycle to balance carbon fixation and catabolism (De Marsac & Houmard, 1993). By moderating levels of reduced TrxA, cyanobacteria control key cellular and metabolic processes, such as carbon fixation, nitrogen metabolism, oxidative stress response, and light harvesting (Blankenship, 2014), and expression of *trxA* transcripts is reduced at lower light levels (Navarro et al., 2000; Pérez-Pérez et al., 2009).

In contrast to the reduced abundance of *Phormidium* in autumn, *Planktothrix* was more abundant in spring and autumn than in summer, suggesting a degree of niche partitioning between these dominant cyanobacteria. The higher abundance of *Planktothrix* in lower-light seasons is consistent with its tolerance to low light levels (Walsby & Schanz, 2002). Further, *Planktothrix* proteins for phycobilisomes and thioredoxin were significantly higher in spring, suggesting higher photosynthetic activity at that time.

In addition to light, sulphide has a strong impact on the physiology of cyanobacteria (Dick et al., 2018), and influences community composition. Seasonal influence of sulphide on MIS mat communities is likely given evidence for stronger sulphur cycling in autumn, including the increased abundance and activity of sulphur cycling bacteria presented here as well as previous measurements of higher sulphide levels in autumn (Kinsman-Costello et al., 2017). *Phormidium* and *Planktothrix* both have genes for sulphide-quinone reductase (*sqr*), which oxidize sulphide for the purpose of AP and/or detoxification (Dick et al., 2018; Voorhies et al., 2012). Our proteomic dataset contained neither SQR proteins nor those from variant photosystem II (*psbA*) genes optimized for low oxygen conditions (Dick et al., 2018; Grim & Dick, 2016), which may have been masked by the much more abundant phycobilisome proteins (which can constitute 40% of cell protein) (Grossman et al., 1995). Lack of protein detection does not imply the absence of function; for example, *Phormidium*'s PsbA was not detected yet we have verified oxygen evolution in the mat (Klatt et al., 2021). However, missing the SQR proteins does preclude inference of the balance of OP and AP photosynthetic modes of these dominant cyanobacteria in the MIS mat, and their relationship to the observed changes in community composition over the seasons.

The increased abundance of SOB and sulphur/sulphate-reducing bacteria in autumn suggests an intensification of the sulphur cycle, which has implications for primary production and O_2 cycling in the cyanobacterial mats (Figure 7). *Beggiatoa* is a dominant sulphur oxidizer in MIS mats, contributing up to 35% of bacterial sequences. It was especially abundant in autumn, when we observed higher abundances of key *Beggiatoa* proteins, such as glyceraldehyde 3-phosphate dehydrogenase involved in the Calvin cycle, an outer membrane protein likely involved in motility (Yu & Kaiser, 2006), and reverse dissimilatory sulphite reductase proteins involved in sulphur oxidation. Lower light levels, as observed in autumn at MIS, also suppress anoxygenic photosynthetic sulphide oxidation, making sulphide more available for chemolithotrophs (Klatt, Meyer, et al., 2016). Taken together, lower light and higher sulphide levels in autumn (Kinsman-Costello et al., 2017), along with increased proteomic and cellular abundance of *Beggiatoa*, suggests that seasonal changes in light availability exerts strong influence on the abundance of sulphide and SOB. *Beggiatoa* is motile and moves vertically to position itself within the gradients of sulphide and oxygen at MIS (Biddanda & Weinke, 2020) and other redox-stratified microbial mats (Jørgensen & Revsbech, 1983). This migration also shades the cyanobacteria on the mat surface, reducing photosynthesis and O_2 production (Dick et al., 2018; Klatt et al., 2021; Klatt, Meyer, et al., 2016). Thus, the seasonal shift towards lower light and more SOB likely hastens declines in rates of photosynthesis and O_2 production.

The 16S rRNA gene and proteomic data indicate that SRB abundance also increased in autumn and suggest interactions with *Beggiatoa* via the sulphur cycle. Network analysis of the 16S rRNA gene time series showed correlated relative abundances of *Beggiatoa* and *Desulfonema*, the most abundant SRB we observed, likely reflecting a metabolic interaction in which sulphide produced through sulphate reduction by *Desulfonema* is used by *Beggiatoa* as an electron donor, as observed in other cyanobacterial mats (Klatt et al., 2020; Stal, 2012). The higher overall abundance of thermodesulfobacterial SRB in summer and autumn (Table S7) is consistent with higher sulphide availability in the mat and sediment later in the year (Kinsman-Costello et al., 2017). However, other putative SRB taxa, such as *Desulfocapsa* and *Desulfotalea*, showed a distinct seasonal pattern, with higher abundance in spring. Proteins from unbinned sequences involved in sulphate reduction (DsrA, DsrC, and ApsR) were observed in summer samples either exclusively or in greater abundance. Thus, SRB taxa are differentially abundant across the seasons, and they are also differentially abundant with depth in mats and underlying sediments (Kinsman-Costello et al., 2017), suggesting that SRB partition niches across both time and space.

In addition to sulphate reduction, *Desulfocapsa* may grow through inorganic sulphur disproportion (Finster et al., 2013; Janssen et al., 1996), and at up to 3.0% relative abundance may play important roles in cycling elemental sulphur, thiosulphate, and sulphite in MIS mats. Sulphur reduction and disproportionation strongly influence photosynthesis and the distribution of cyanobacteria and SOBs in other mat systems (Dick et al., 2018; Klatt et al., 2020; Stal, 2012).

Proteins from other taxa provided additional evidence for seasonal changes in biogeochemistry and metabolism in MIS mats. Diatoms, which likely play important roles in nitrogen cycling within MIS mats (Merz et al., 2021), contributed nearly 16% of peptide spectra in autumn and spring. A carbon fixation protein from another putative phototroph, the purple nonsulphur bacterium *Rhodoferax* (Kaden et al., 2014; Madigan et al., 2000), was highly abundant in summer, suggesting that it may contribute to primary production. Finally, an outer membrane protein from *Methylococcaceae*, a putative methanotroph, was enriched in autumn samples, consistent with more reducing redox conditions within mats in the autumn.

Variation in measured protein relative abundances could reflect both seasonal changes in community composition and changes in protein expression levels within individual taxa. *Phormidium's* growth during the optimal conditions experienced in summer is reflected in its high relative abundance in both the proteomic and 16S rRNA gene data from those samples. However, in other cases, relative abundances from proteome profiles were not aligned with those from 16S rRNA gene surveys. *Planktothrix* proteins were more often observed in spring than in other seasons, but *Planktothrix* was not the most abundant cyanobacterium in 16S rRNA gene datasets in spring due to the dominance of *Phormidium*. On the other hand, *Planktothrix's* higher relative abundance of 16S rRNA genes in autumn is more likely a consequence of lower *Phormidium* abundance. In another example, *Beggiatoa* and other SOB were present in the bacterial community throughout the year, but the higher abundance of their proteins in autumn likely reflects higher activity and growth.

CONCLUSION

This study showed that seasonal changes in irradiance and water chemistry are accompanied by large shifts in microbial community structure and function in the microbial mat of MIS. While the current data cannot conclusively disentangle the effects of light versus water chemistry, the proteomic data suggest that light quantity and quality were an important driver of seasonal changes in community composition and metabolism. In addition to changes in the phototrophic community, seasonal shifts in the community of SRB and increased abundance of sulphur-oxidizing *Beggiatoa* in autumn supports the hypothesis that lower light levels lead to an intensified sulphur cycle, perhaps via shifts in photosynthetic rates and/or the balance of OP and AP. The increased autumn abundance of *Beggiatoa* likely has feedback effects on light available to phototrophs as these SOB cover and compete with the cyanobacteria (Biddanda & Weinke, 2020; Klatt et al., 2020, 2021; Klatt, Meyer, et al., 2016). These insights have implications for how seasonality affects the cycling of carbon, sulphur, and oxygen in cyanobacterial mats, and may inform understanding of controls on O_2 production in widespread redox-stratified mats of the Proterozoic. The results are also relevant to the vulnerability of rare microbial mat ecosystems to environmental change in the modern world; links between microbial composition and function and light and chemistry/hydrology are also likely to manifest in recent anthropogenic environmental change such as changes in water clarity due to invasive dreissenid mussels (Binding et al., 2007) and hydrological shifts associated with climate change, including rapidly fluctuating Great Lakes water levels (Gronewold & Rood, 2019) and changes in groundwater flux.

CONFLICT OF INTEREST STATEMENT

All authors declare no conflict of interest.

DATA AVAILABILITY STATEMENT

The 16S rRNA gene amplicon sequencing data that support the findings of this study are openly available in NCBI Sequence Read Archive (https://www.ncbi.nlm.nih.gov/bioproject/PRJNA305364), accessible via Traces SRP067517 within BioProject PRJNA305364. Proteomic mass spectral data for this study are available via ProteomeXchange under accession number PXD031126 and the MassIVE repository (https://massive.ucsd.edu/) under accession number MSV000088706.

ORCID

Sharon L. Grim https://orcid.org/0000-0003-4215-7519

Phoebe Aron https://orcid.org/0000-0002-4700-5445

Naomi E. Levin https://orcid.org/0000-0001-5703-3717

Lauren Kinsman-Costello https://orcid.org/0000-0002-9168-8677

Jacob R. Waldbauer https://orcid.org/0000-0002-0338-6143

Gregory J. Dick https://orcid.org/0000-0001-7666-6288

REFERENCES

Afgan, E., Baker, D., Batut, B., van den Beek, M., Bouvier, D., Čech, M. et al. (2018) The Galaxy platform for accessible, reproducible and collaborative biomedical analyses: 2018 update. *Nucleic Acids Research*, 46(W1), W537–W544. Available from: https://doi.org/10.1093/nar/gky379

Aguilera, Á., Suominen, S., Pétursdóttir, S., Olgudóttir, E., Guðmundsdóttir, E.E., Altamirano, M. et al. (2020) Physiological plasticity of high-temperature intertidal cyanobacterial microbial mats to temperature and salinity: daily and seasonal in situ photosynthetic performance. *European Journal of Phycology*, 55(2), 223–233. Available from: https://doi.org/10.1080/09670262.2019.1690165

Al-Najjar, M.A.A., Ramette, A., Kühl, M., Hamza, W., Klatt, J.M. & Polerecky, L. (2014) Spatial patterns and links between microbial community composition and function in cyanobacterial mats. *Frontiers in Microbiology*, 5, 406. Available from: https://doi.org/10.3389/fmicb.2014.00406

Baskaran, M., Novell, T., Nash, K., Ruberg, S.A., Johengen, T., Hawley, N. et al. (2016) Tracing the seepage of subsurface sinkhole vent waters into Lake Huron using radium and stable isotopes of oxygen and hydrogen. *Aquatic Geochemistry*, 22(4), 349–374. Available from: https://doi.org/10.1007/s10498-015-9286-7

Biddanda, B.A., McMillan, A.C., Long, S.A., Snider, M.J. & Weinke, A.D. (2015) Seeking sunlight: rapid phototactic motility of filamentous mat-forming cyanobacteria optimize photosynthesis and enhance carbon burial in Lake Huron's submerged sinkholes. *Frontiers in Microbiology*, 6, 930. Available from: https://doi.org/10.3389/fmicb.2015.00930

Biddanda, B.A. & Weinke, A.D. (2020) Extant mat world analog microbes synchronize migration to a diurnal tempo. *AGU Advances*. Available from: https://doi.org/10.1002/essoar.10502762.1

Binding, C.E., Jerome, J.H., Bukata, R.P. & Booty, W.G. (2007) Trends in water clarity of the lower Great Lakes from remotely sensed aquatic color. *Journal of Great Lakes Research*, 33(4), 828–841. Available from: https://doi.org/10.3394/0380-1330(2007)33[828:TIWCOT]2.0.CO;2

Blankenship, R.E. (2014) *Molecular mechanisms of photosynthesis*, 1st edition. Blackwell Science Ltd.

Bolhuis, H., Cretoiu, M.S. & Stal, L.J. (2014) Molecular ecology of microbial mats. *FEMS Microbiology Ecology*, 90, 335–350. Available from: https://doi.org/10.1111/1574-6941.12408

Bowen, G.J., Kennedy, C.D., Henne, P.D. & Zhang, T. (2012) Footprint of recycled water subsidies downwind of Lake Michigan. *Ecosphere*, 3, 1–16.

Bryant, D.A. (1982) Phycoerythrocyanin and Phycoerythrin: properties and occurrence in cyanobacteria. *Journal of General Microbiology*, 128, 835–844.

Camacho, A., Rochera, C., Silvestre, J.J., Vicente, E. & Hahn, M.W. (2005) Spatial dominance and inorganic carbon assimilation by conspicuous autotrophic biofilms in a physical and chemical gradient of a cold sulfurous spring: the role of differential ecological strategies. *Microbial Ecology*, 50(2), 172–184. Available from: https://doi.org/10.1007/s00248-004-0156-x

Canfield, D.E. & Des Marais, D.J. (1991) Aerobic sulfate reduction in microbial mats. *Science*, 251, 1471–1473. Available from: https://doi.org/10.1126/science.11538266

Cardoso, D.C., Cretoiu, M.S., Stal, L.J. & Bolhuis, H. (2019) Seasonal development of a coastal microbial mat. *Scientific Reports*, 9, 9035. Available from: https://doi.org/10.1038/s41598-019-45490-8

Cobley, J.G., Clark, A.C., Weerasurya, S., Queseda, F.A., Xiao, J.Y., Bandrapali, N. et al. (2002) CpeR is an activator required for expression of the phycoerythrin operon (*cpeBA*) in the cyanobacterium *Fremyella diplosiphon* and is encoded in the phycoerythrin linker-polypeptide operon (*cpeCDESTR*). *Molecular Microbiology*, 44, 1517–1531.

Cohen, Y., Jørgensen, B.B., Padan, E. & Shilo, M. (1975) Sulphide-dependent anoxygenic photosynthesis in the cyanobacterium *Oscillatoria limnetica*. *Nature*, 257(5526), 489–492. Available from: https://doi.org/10.1038/257489a0

Coplen, T.B. (1996) New guidelines for reporting stable hydrogen, carbon, and oxygen isotope-ratio data. *Geochimica et Cosmochimica Acta*, 60, 3359–3360.

Cory, R.M., Davis, T.W., Dick, G.J., Johengen, T., Denef, V.J., Berry, M.A. et al. (2016) Seasonal dynamics in dissolved organic matter, hydrogen peroxide, and cyanobacterial blooms in Lake Erie. *Frontiers in Marine Science*, 3, 3815. Available from: https://doi.org/10.3389/fmars.2016.00054

Craig, H. (1961) Isotopic variations in meteoric waters. *Science*, 133(3465), 1702–1703. Available from: https://www.science.org/doi/10.1126/science.133.3465.1702

de Beer, D., Weber, M., Chennu, A., Hamilton, T.L., Lott, C., Macalady, J. et al. (2017) Oxygenic and anoxygenic photosynthesis in a microbial mat from an anoxic and sulfidic spring. *Environmental Microbiology*, 19(3), 1251–1265. Available from: https://doi.org/10.1111/1462-2920.13654

De Marsac, N.T. & Houmard, J. (1993) Adaptation of cyanobacteria to environmental stimuli: new steps towards molecular mechanisms. *FEMS Microbiology Reviews*, 10, 119–189.

Decelle, J., Romac, S., Stern, R.F., Bendif, E.M., Zingone, A., Audic, S. et al. (2015) PhytoREF: a reference database of the plastidial 16S rRNA gene of photosynthetic eukaryotes with curated taxonomy. *Molecular Ecology Resources*, 15(6), 1435–1445. Available from: https://doi.org/10.1111/1755-0998.12401

Dick, G.J., Grim, S.L. & Klatt, J.M. (2018) Controls on O2 production in cyanobacterial Mats and Implications for Earth's oxygenation. *Annual Review of Earth and Planetary Sciences*, 46(1), 123–147. Available from: https://doi.org/10.1146/annurev-earth-082517-010035

Dillon, M.L., Hawes, I., Jungblut, A.D., Mackey, T.J., Eisen, J.A., Doran, P.T. et al. (2020a) Energetic and environmental constraints on the community structure of benthic microbial Mats in Lake Fryxell, Antarctica. *FEMS Microbiology Ecology*, 96(2), fix207. Available from: https://doi.org/10.1093/femsec/fiz207

Dillon, M.L., Hawes, I., Jungblut, A.D., Mackey, T.J., Eisen, J.A., Doran, P.T. et al. (2020b) Environmental control on the distribution of metabolic strategies of benthic microbial mats in Lake Fryxell, Antarctica. *PLoS One*, 15(4), e0231053. Available from: https://doi.org/10.1371/journal.pone.0231053

Erde, J., Loo, R.R.O. & Loo, J.A. (2014) Enhanced FASP (eFASP) to increase proteome coverage and sample recovery for quantitative proteomic experiments. *Journal of Proteome Research*, 13(4), 1885–1895. Available from: https://doi.org/10.1021/pr4010019

Eren, A.M., Esen, O.C., Quince, C., Vineis, J.H., Morrison, H.G., Sogin, M.L. et al. (2015) Anvi'o: an advanced analysis and visualization platform for 'omics data. *PeerJ*, 3(358), e1319. Available from: https://doi.org/10.7717/peerj.1319

Eren, A.M., Maignien, L., Sul, W.J., Murphy, L.G., Grim, S.L., Morrison, H.G. et al. (2013) Oligotyping: differentiating between closely related microbial taxa using 16S rRNA gene data. *Methods in Ecology and Evolution*, 4(12), 1111–1119. Available from: https://doi.org/10.1111/2041-210X.12114

Eren, A.M., Morrison, H.G., Lescault, P.J., Reveillaud, J., Vineis, J.H. & Sogin, M.L. (2014) Minimum entropy decomposition: unsupervised oligotyping for sensitive partitioning of high-throughput marker gene sequences. *The ISME Journal*, 1–12, 968–979. Available from: https://doi.org/10.1038/ismej.2014.195

Excoffier, L., Smouse, P.E. & Quattro, J.M. (1992) Molecular variance inferred from metric distances among DNA haplotypes: application to human mitochondrial DNARestriction data. *Genetics*, 131, 479–491.

Fahnenstiel, G.L. & Carrick, H.J. (1991) Phototrophic picoplankton in lakes Huron and Michigan: abundance, distribution, composition, and contribution to biomass and production. *Canadian Journal of Fisheries and Aquatic Sciences*, 49, 379–388. Available from: https://doi.org/10.1139/f92-043

Falkowski, P.G. & LaRoche, J. (1991) Acclimation to spectral irradiance in algae. *Journal of Phycology*, 27(1), 8–14. Available from: https://doi.org/10.1111/j.0022-3646.1991.00008.x

Faust, K. & Raes, J. (2012) Microbial interactions: from networks to models. *Nature Publishing Group*, 10(8), 538–550. Available from: https://doi.org/10.1038/nrmicro2832

Faust, K. & Raes, J. (2016) CoNet app: inference of biological association networks using Cytoscape. *F1000Research*, 5, 1519. Available from: https://doi.org/10.12688/f1000research.9050.2

Finster, K.W., Kjeldsen, K.U., Kube, M., Reinhardt, R., Mussmann, M., Amann, R. et al. (2013) Complete genome sequence of *Desulfocapsa sulfexigens*, a marine deltaproteobacterium specialized in disproportionating inorganic sulfur compounds. *Standards in Genomic Sciences*, 8(1), 58–68. Available from: https://doi.org/10.4056/sigs.3777412

Georgopoulos, C. & Welch, W.J. (1993) Role of the major heat shock proteins as molecular chaperones. *Annual Review of Cellular Biology*, 3, 601–634.

Green, B.R. (2011) Chloroplast genomes of photosynthetic eukaryotes. *The Plant Journal*, 66(1), 34–44. Available from: https://doi.org/10.1111/j.1365-313X.2011.04541.x

Grim, S.L. & Dick, G.J. (2016) Photosynthetic versatility in the genome of *Geitlerinema* sp. PCC 9228 (formerly *Oscillatoria limnetica* "solar Lake"), a model Anoxygenic photosynthetic cyanobacterium. *Frontiers in Microbiology*, 7(590), 1144. Available from: https://doi.org/10.3389/fmicb.2016.01546

Grim, S.L., Voorhies, A.A., Biddanda, B.A., Jain, S., Nold, S.C., Green, R. et al. (2021) Omics-inferred partitioning and expression of diverse biogeochemical functions in a low-O2 cyanobacterial mat community. *mSystems*, 6, e0104221. Available from: https://doi.org/10.1128/mSystems.01042-21&domain=pdf&date_stamp=2021-12-21

Gronewold, A.D. & Rood, R.B. (2019) Recent water level changes across Earth's largest lake system and implications for future variability. *Journal of Great Lakes Research*, 45(1), 1–3. Available from: https://doi.org/10.1016/j.jglr.2018.10.012

Grossman, A.R., Bhaya, D. & Apt, K.E. (1995) Light-harvesting complexes in oxygenic photosynthesis: diversity, control, and evolution. *Annual Review of Genetics*, 29(1), 231–288. Available from: https://doi.org/10.1146/annurev.ge.29.120195.001311

Guan, X., Qin, S., Zhao, F., Zhang, X. & Tang, X. (2007) Phycobilisomes linker family in cyanobacterial genomes: divergence and evolution. *International Journal of Biological Sciences*, 3, 434–445.

Hamilton, T.L., Bryant, D.A. & Macalady, J.L. (2016) The role of biology in planetary evolution: cyanobacterial primary production in low-oxygen Proterozoic oceans. *Environmental Microbiology*, 18(2), 325–340. Available from: https://doi.org/10.1111/1462-2920.13118

Hamilton, T.L., Klatt, J.M., de Beer, D. & Macalady, J.L. (2018) Cyanobacterial photosynthesis under sulfidic conditions: insights from the isolate *Leptolyngbya* sp. strain hensonii. *The ISME Journal*, 12(2), 568–584. Available from: https://doi.org/10.1038/ismej.2017.193

Hawes, I. & Schwarz, A.M.J. (2001) Absorption and utilization of irradiance by cyanobacterial mats in two ice-covered antarctic lakes with contrasting light climates. *Journal of Phycology*, 37(1), 5–15. Available from: https://doi.org/10.1046/j.1529-8817.1999.014012005.x

Hihara, Y., Kamei, A., Kanehisa, M., Kaplan, A. & Ikeuchi, M. (2001) DNA microarray analysis of cyanobacterial gene expression during acclimation to high light. *The Plant Cell*, 13, 793–806.

Hoehler, T.M., Bebout, B.M. & Des Marais, D.J. (2001) The role of microbial mats in the production of reduced gases on the early Earth. *Nature*, 412(6844), 324–327. Available from: https://doi.org/10.1038/35085554

Huse, S.M., Dethlefsen, L., Huber, J.A., Welch, D.M., Relman, D.A. & Sogin, M.L. (2008) Exploring microbial diversity and taxonomy using SSU rRNA hypervariable tag sequencing. *PLoS Genetics*, 4(11), e1000255. Available from: https://doi.org/10.1371/journal.pgen.1000255

Jahn, M., Vialas, V., Karlsen, J., Maddalo, G., Edfors, F., Forsström, B. et al. (2018) Growth of cyanobacteria is constrained by the abundance of light and carbon assimilation proteins. *CellReports*, 25(2), 478–486.e8. Available from: https://doi.org/10.1016/j.celrep.2018.09.040

Janssen, P.H., Schuhmann, A., Bak, F. & Liesack, W. (1996) Disproportionation of inorganic sulfur compounds by the sulfate-reducing bacterium *Desulfocapsa thiozymogenes* gen. Nov., sp. nov. *Archives of Microbiology*, 166(3), 184–192. Available from: https://doi.org/10.1007/s002030050374

Jasechko, S., Gibson, J.J. & Edwards, T.W.D. (2014) Stable isotope mass balance of the Laurentian Great Lakes. *Journal of Great Lakes Research*, 40(2), 336–346. Available from: https://doi.org/10.1016/j.jglr.2014.02.020

Jørgensen, B.B., Cohen, Y. & Des Marais, D.J. (1987) Photosynthetic action spectra and adaptation to spectral light-distribution in a benthic cyanobacterial mat. *Applied and Environmental Microbiology*, 53(4), 879–886.

Jørgensen, B.B., Cohen, Y. & Revsbech, N.P. (1986) Transition from Anoxygenic to oxygenic photosynthesis in a *Microcoleus chthonoplastes* cyanobacterial mat. *Applied and Environmental Microbiology*, 51(2), 408–417.

Jørgensen, B.B. & Revsbech, N.P. (1983) Colorless sulfur bacteria, *Beggiatoa* spp. and *Thiovulum* spp., in O2 and H2S microgradients. *Applied and Environmental Microbiology*, 45(4), 1261–1270.

Kaden, R., Sproer, C., Beyer, D. & Krolla-Sidenstein, P. (2014) *Rhodoferax saidenbachensis* sp. nov., a psychrotolerant, very slowly

growing bacterium within the family *Comamonadaceae*, proposal of appropriate taxonomic position of *Albidiferax ferriraducens* strain T118T in the genus *Rhodoferax* and emended description of the genus *Rhodoferax*. *International Journal of Systematic and Evolutionary Microbiology*, 64(Pt 4), 1186–1193. Available from: https://doi.org/10.1099/ijs.0.054031-0

Kinsman-Costello, L.E., Sheik, C.S., Sheldon, N.D., Allen Burton, G., Costello, D.M., Marcus, D. et al. (2017) Groundwater shapes sediment biogeochemistry and microbial diversity in a submerged great Lake sinkhole. *Geobiology*, 15(2), 225–239. Available from: https://doi.org/10.1111/gbi.12215

Klatt, J.M., Al-Najjar, M.A.A., Yilmaz, P., Lavik, G., de Beer, D. & Polerecky, L. (2015) Anoxygenic photosynthesis controls oxygenic photosynthesis in a cyanobacterium from a sulfidic spring. *Applied and Environmental Microbiology*, 81(6), 2025–2031. Available from: https://doi.org/10.1128/AEM.03579-14

Klatt, J.M., Chennu, A., Arbic, B.K., Biddanda, B.A. & Dick, G.J. (2021) Possible link between Earth's rotation rate and oxygenation. *Nature Geoscience*, 1–19, 564–570. Available from: https://doi.org/10.1038/s41561-021-00784-3

Klatt, J.M., de Beer, D., Häusler, S. & Polerecky, L. (2016) Cyanobacteria in sulfidic spring microbial mats can perform oxygenic and Anoxygenic photosynthesis simultaneously during an entire diurnal period. *Frontiers in Microbiology*, 7(116), 440. Available from: https://doi.org/10.3389/fmicb.2016.01973

Klatt, J.M., Gomez-Saez, G.V., Meyer, S., Ristova, P.P., Yilmaz, P., Granitsiotis, M.S. et al. (2020) Versatile cyanobacteria control the timing and extent of sulfide production in a Proterozoic analog microbial mat. *The ISME Journal*, 1–14, 3024–3037. Available from: https://doi.org/10.1038/s41396-020-0734-z

Klatt, J.M., Meyer, S., Häusler, S., Macalady, J.L., de Beer, D. & Polerecky, L. (2016) Structure and function of natural sulphide-oxidizing microbial mats under dynamic input of light and chemical energy. *The ISME Journal*, 10(4), 921–933. Available from: https://doi.org/10.1038/ismej.2015.167

Kozich, J.J., Westcott, S.L., Baxter, N.T., Highlander, S.K. & Schloss, P.D. (2013) Development of a dual-index sequencing strategy and curation pipeline for analyzing amplicon sequence data on the MiSeq Illumina sequencing platform. *Applied and Environmental Microbiology*, 79(17), 5112–5120. Available from: https://doi.org/10.1128/AEM.01043-13

Lenton, T.M. & Daines, S.J. (2017) Matworld – the biogeochemical effects of early life on land. *New Phytologist*, 215(2), 531–537. Available from: https://doi.org/10.1111/nph.14338

Lionard, M., Péquin, B., Lovejoy, C. & Vincent, W.F. (2012) Benthic cyanobacterial mats in the high arctic: multi-layer structure and fluorescence responses to osmotic stress. *Frontiers in Microbiology*, 3, 140. Available from: https://doi.org/10.3389/fmicb.2012.00140

Lyons, T.W., Reinhard, C.T. & Planavsky, N.J. (2014) The rise of oxygen in Earth's early ocean and atmosphere. *Nature*, 506(7488), 307–315. Available from: https://doi.org/10.1038/nature13068

Mackey, T.J., Sumner, D.Y., Hawes, I. & Jungblut, A.D. (2017) Morphological signatures of microbial activity across sediment and light microenvironments of Lake Vanda, Antarctica. *Sedimentary Geology*, 361(C), 82–92. Available from: https://doi.org/10.1016/j.sedgeo.2017.09.013

Madigan, M.T., Jung, D.O., Woese, C.R. & Achenbach, L.A. (2000) *Rhodoferax antarcticus* sp. nov., a moderately psychrophilic purple nonsulfur bacterium isolated from an Antarctic microbial mat. *Archives of Microbiology*, 173(4), 269–277. Available from: https://doi.org/10.1007/s002030000140

McLaren, M.R., Nearing, J.T., Willis, A.D., Lloyd, K.G. & Callahan, B.J. (2022) Implications of taxonomic bias for microbial differential-abundance analysis. bioRxiv, 2022.08.19.504330.

Merz, E., Dick, G.J., de Beer, D., Grim, S., Hübener, T., Littmann, S. et al. (2021) Nitrate respiration and diel migration patterns of

diatoms are linked in sediments underneath a microbial mat. *Environmental Microbiology*, 23(3), 1422–1435. Available from: https://doi.org/10.1111/1462-2920.15345

Moore, L.R., Rocap, G. & Chisholm, S.W. (1998) Physiology and molecular phylogeny of coexisting Prochlorococcus ecotypes. *Nature*, 393(6684), 464–467. Available from: https://doi.org/10.1038/30965

Moorhead, D.L., Wolf, C.F. & Wharton, R.A. (1997) Impact of light regimes on productivity patterns of benthic microbial mats in an antarctic lake: a modeling study. *Limnology and Oceanography*, 42(7), 1561–1569. Available from: https://doi.org/10.4319/lo.1997.42.7.1561

Navarro, F., Martín-Figueroa, E. & Florencio, F.J. (2000) Electron transport controls transcription of the thioredoxin gene (*trxA*) in the cyanobacterium *Synechocystis* sp. PCC 6803. *Plant Molecular Biology*, 43(1), 23–32.

Oberhaus, L., Briand, J.F., Leboulanger, C., Jacquet, S. & Humbert, J.F. (2007) Comparative effects of the quality and quantity of light and temperature on the growth of *Planktothrix agardhii* and *P. rubescens*. *Journal of Phycology*, 43(6), 1191–1199. Available from: https://doi.org/10.1111/j.1529-8817.2007.00414.x

Paradis, E. (2010) Pegas: an R package for population genetics with an integrated-modular approach. *Bioinformatics*, 26(3), 419–420. Available from: https://doi.org/10.1093/bioinformatics/btp696

Pérez-Pérez, M.E., Martín-Figueroa, E. & Florencio, F.J. (2009) Photosynthetic regulation of the cyanobacterium *Synechocystis* sp. PCC 6803 Thioredoxin system and functional analysis of TrxB (Trx *x*) and TrxQ (Trx *y*) Thioredoxins. *Molecular Plant*, 2(2), 270–283. Available from: https://doi.org/10.1093/mp/ssn070

Pinckney, J., Paerl, H.W. & Fitzpatrick, M. (1995) Impacts of seasonality and nutrients on microbial mat community structure and function. *Marine Ecology Progress Series*, 123, 207–216.

Pruesse, E., Quast, C., Knittel, K., Fuchs, B.M., Ludwig, W., Peplies, J. et al. (2007) SILVA: a comprehensive online resource for quality checked and aligned ribosomal RNA sequence data compatible with ARB. *Nucleic Acids Research*, 35(21), 7188–7196. Available from: https://doi.org/10.1093/nar/gkm864

R Core Team. (2015) *R: a language and environment for statistical computing*. Vienna, Austria: R Foundation for Statistical Computing. https://www.r-project.org/

Richardson, L.L. & Castenholz, R.W. (1987) Diel vertical movements of the cyanobacterium oscillatoria-terebriformis in a sulfide-rich hot-spring microbial mat. *Applied and Environmental Microbiology*, 53(9), 2142–2150.

Rinalducci, S., Roepstorff, P. & Zolla, L. (2008) De novosequence analysis and intact mass measurements for characterization of phycocyanin subunit isoforms from the blue-green alga *Aphanizomenon flos-aquae*. *Journal of Mass Spectrometry*, 44(4), 503–515. Available from: https://doi.org/10.1002/jms.1526

RStudio Team. (2014) *RStudio: Integrated Development for R*. Boston: RStudio Inc. http://www.rstudio.com/

Ruberg, S.A., Kendall, S.T. & Biddanda, B.A. (2008) Observations of the Middle Island sinkhole in Lake Huron–a unique hydrogeologic and glacial creation of 400 million years. *Marine Technology Society Journal*, 42(4), 12–21. Available from: https://doi.org/10.4031/002533208787157633

Schloss, P.D., Westcott, S.L., Ryabin, T., Hall, J.R., Hartmann, M., Hollister, E.B. et al. (2009) Introducing mothur: open-source, platform-independent, community-supported software for describing and comparing microbial communities. *Applied and Environmental Microbiology*, 75(23), 7537–7541. Available from: https://doi.org/10.1128/AEM.01541-09

Seekatz, A.M., Theriot, C.M., Molloy, C.T., Wozniak, K.L., Bergin, I.L. & Young, V.B. (2015) Fecal microbiota transplantation eliminates Clostridium difficile in a murine model of relapsing

disease. *Infection and Immunity*, 83(10), 3838–3846. Available from: https://doi.org/10.1128/IAI.00459-15

Snider, M.J., Biddanda, B.A., Lindback, M., Grim, S.L. & Dick, G.J. (2017) Versatile photophysiology of compositionally similar cyanobacterial mat communities inhabiting submerged sinkholes of Lake Huron. *Aquatic Microbial Ecology*, 79(1), 63–78. Available from: https://doi.org/10.3354/ame01813

Stal, L.J. (2012) Cyanobacterial Mats and Stromatolites. In: Whitton, B.A. (Ed.) *Ecology of cyanobacteria II*. Dordrecht: Springer Netherlands, pp. 65–125. Available from: https://doi.org/10.1007/978-94-007-3855-3_4

Stomp, M., Huisman, J., De Jongh, F., Veraart, A.J., Gerla, D., Rijkeboer, M. et al. (2004) Adaptive divergence in pigment composition promotes phytoplankton biodiversity. *Nature*, 432(7013), 104–107. Available from: https://doi.org/10.1038/nature03044

Sumner, D.Y., Hawes, I., Mackey, T.J., Jungblut, A.D. & Doran, P.T. (2015) Antarctic microbial mats: a modern analog for Archean lacustrine oxygen oases. *Geology*, 43(10), 887–890. Available from: https://doi.org/10.1130/G36966.1

Teske, A., Ramsing, N.B., Habicht, K., Fukui, M., Küver, J., Jørgensen, B.B. et al. (1998) Sulfate-reducing bacteria and their activities in cyanobacterial mats of solar Lake (Sinai, Egypt). *Applied and Environmental Microbiology*, 64(8), 2943–2951.

Voorhies, A.A., Biddanda, B.A., Kendall, S.T., Jain, S., Marcus, D.N., Nold, S.C. et al. (2012) Cyanobacterial life at low O2: community genomics and function reveal metabolic versatility and extremely low diversity in a Great Lakes sinkhole mat. *Geobiology*, 10(3), 250–267. Available from: https://doi.org/10.1111/j.1472-4669.2012.00322.x

Voorhies, A.A., Eisenlord, S.D., Marcus, D.N., Duhaime, M.B., Biddanda, B.A., Cavalcoli, J.D. et al. (2016) Ecological and genetic interactions between cyanobacteria and viruses in a low-oxygen mat community inferred through metagenomics and metatranscriptomics. *Environmental Microbiology*, 18(2), 358–371. Available from: https://doi.org/10.1111/1462-2920.12756

Waldbauer, J.R., Zhang, L., Rizzo, A. & Muratore, D. (2017) diDO-IPTL: a peptide-labeling strategy for precision quantitative proteomics. *Analytical Chemistry*, 89(21), 11498–11504. Available from: https://doi.org/10.1021/acs.analchem.7b02752

Walsby, A.E. & Schanz, F. (2002) Light-dependent growth rate determines changes in the population of Planktothrix rubescens over the annual cycle in Lake Zürich, Switzerland. *New Phytologist*, 154(3), 671–687. Available from: https://doi.org/10.1046/j.1469-8137.2002.00401.x

Ward, D.M., Bateson, M.M., Ferris, M.J., Kuhl, M., Wieland, A., Koeppel, A. et al. (2006) Cyanobacterial ecotypes in the microbial mat community of mushroom spring (Yellowstone National Park, Wyoming) as species-like units linking microbial community composition, structure and function. *Philosophical Transactions of the Royal Society B: Biological Sciences*, 361(1475), 1997–2008. Available from: https://doi.org/10.1098/rstb.2006.1919

Yousef, F., Shuchman, R., Sayers, M., Fahnenstiel, G. & Henareh, A. (2017) Water clarity of the upper Great Lakes: tracking changes between 1998-2012. *Journal of Great Lakes Research*, 43(2), 239–247. Available from: https://doi.org/10.1016/j.jglr.2016.12.002

Yu, R. & Kaiser, D. (2006) Gliding motility and polarized slime secretion. *Molecular Microbiology*, 63(2), 454–467. Available from: https://doi.org/10.1111/j.1365-2958.2006.05536.x

SUPPORTING INFORMATION

Additional supporting information can be found online in the Supporting Information section at the end of this article.